

# An efficient four node degenerated shell element based on the assumed covariant strain

Chang-Koon Choi<sup>†</sup> and Jong-Gyun Paik<sup>‡</sup>

Department of Civil Engineering, Korea Advanced Institute of Science and Technology,  
Taejeon 305-701, Korea

**Abstract.** This paper proposes a new four node degenerated shell element. In the formulation of the new element, the assumed covariant shear strains are used to avoid the shear locking problem, and the assumed covariant membrane strains are applied to alleviate the membrane locking problem and also to improve the membrane bending performance. The assumed covariant strains are obtained from the covariant strain field defined with respect to the element natural coordinate system. This formulation enables us to obtain a shell element, which does not produce spurious singular modes, avoids locking phenomena, and excels in calculation efficiency. Several examples in this paper indicate that, despite its simplicity, the achieved accuracy and convergence are satisfactory.

**Key words:** assumed strain; degenerated shell element; shear locking; membrane locking; covariant; natural coordinate line; membrane bending.

---

## 1. Introduction

The degenerated shell element has been proven to be a successful general shell element in the thin and moderately thick plate and shell analysis. The basic assumptions employed in degenerated shell elements allow the transverse shear deformation and the isoparametric representation of kinematics of deformation. It thus can be applied to the finite element modeling of the arbitrary shell geometry without using any particular shell theory. The original degenerated shell element (Ahmad et al. 1970) gives reasonably good results for moderately thick shells. However, the performance of the element deteriorates rapidly as the shell thickness becomes thin (Zienkiewicz et al. 1971).

This phenomenon is called *locking*. Two different types of locking effects in thin shell elements were identified by Lee et al. (1978) and Belytschko et al. (1985). First type of locking, i. e. the shear locking, is associated with the overconstraining effect of the condition of zero transverse shear strain energy on the assumed displacement field for thin shells. Secondly, the membrane locking is due to the overconstraining effect of the condition of zero membrane strains for curved shells. These problems are more subtle for lower-order elements which are often preferred in many analyses, in particular nonlinear problems, because of the simplicity of element and the easiness of modeling. To alleviate these deficiencies, several methods have

---

<sup>†</sup> Professor

<sup>‡</sup> Graduate Student

been proposed by many investigators in the past such as the selective and reduced integration schemes (Parisch 1979, Hughes et al. 1978), heterosis elements (Hughes and Cohen 1978), stabilization methods (Belytschko et al. 1989), and discrete Kirchhoff elements, etc.

With the aforementioned developments, it is possible to obtain a number of successful  $C^0$  displacement-based degenerated shell elements. These approaches, however, provide a number of distinct limitations. The selective or reduced integration scheme is not always successful in overcoming the locking problem and thus the resulting solutions may be overstiff for problems with highly constrained boundaries when coarse meshes are used. Furthermore, for the problems with lightly constrained boundaries, these schemes may engender the rank deficiency (Parisch 1979, Belytschko et al. 1989). Heterosis elements exhibit the overstiffening effect for the problem with irregular mesh (Choi and Kim 1989). The stabilization methods involve certain parameters which still lack appropriate physical interpretations. Discrete Kirchhoff elements do not include the transverse shear deformation effect due to the Kirchhoff hypothesis and therefore still circumvent the membrane locking. Thus, there is still no general consensus in favor of a particular approach to avoid the locking problems due to its aforementioned inherent limitations.

Lately, Dvorkin and Bathe (Dvorkin and Bathe 1984, Bathe and Dvorkin 1986), Park and Stanley (Stanley 1985, Park and Stanley 1986), Huang and Hinton (Huang and Hinton 1986, Huang 1987) and Jang and Pinsky (Jang and Pinsky 1987) have developed various elements based on the assumed strain methods to solve the locking problems. The first two elements (Dvorkin and Bathe's and Park and Stanley's) seem to be among the best available 4 node elements. The four node element proposed by Park and Stanley (1985) uses the assumed strains for all the strain components, i.e. membrane, bending and transverse shear strains. But because the assumed bending strain cannot satisfy the rigid body motion condition, this element locks the solution for a pinched hemispherical shell problem unless the reduced one-point integration is invoked. And this element has a restriction on transverse shear deformations and the application to the laminated composite shell because of the thickness pre-integration. Another four node element developed by Dvorkin and Bathe (1984) uses assumed strains only for the transverse shear components, but not for the membrane components because the membrane strain cannot be decoupled from the in-plane strain in their element. Therefore, this element is still overstiff for the membrane behavior.

In this paper, a simple and efficient four node degenerated shell element which overcomes aforementioned drawbacks is proposed. This element uses the assumed strain concept in terms of covariant strains referred to the element natural coordinate system. In formulation of the element, the assumed shear strains are used to avoid the shear locking. The covariant membrane strains are separated from the covariant in-plane strains which consist of the combination of the membrane and bending strains by mid-surface interpolation. With these separated strains, it is now possible to use the assumed membrane strains to alleviate the membrane locking by eliminating the violation in the rigid body motion condition caused by applying assumed bending strains.

Since this element is used under the three dimensional stress-strain condition, this element is applicable to both thin and thick shells and can be easily implemented into the existing finite element analysis program by minimum modification. A brief comparison of major four node elements and the element proposed in this study is given in Table 1.

Numerical examples are presented to evaluate the performance of the new element developed. The proposed element has no hourglass modes and the numerical results indicate that

this element has a rapid convergence, provides a reasonable accuracy for the stresses, and also improves the membrane bending behavior of the shell.

Table 1 Comparison of the 4-node assumed strain elements

		Bathe & Dvorkin	Park & Stanley	This study
Strain	Membrane	Displacement Model	Assumed Strain	Assumed Strain
	Bending		Assumed Strain	Displacement Model
	Transverse shear	Assumed Strain	Assumed Strain	Assumed Strain
Application		Thin or Thick	Thin	Thin or Thick

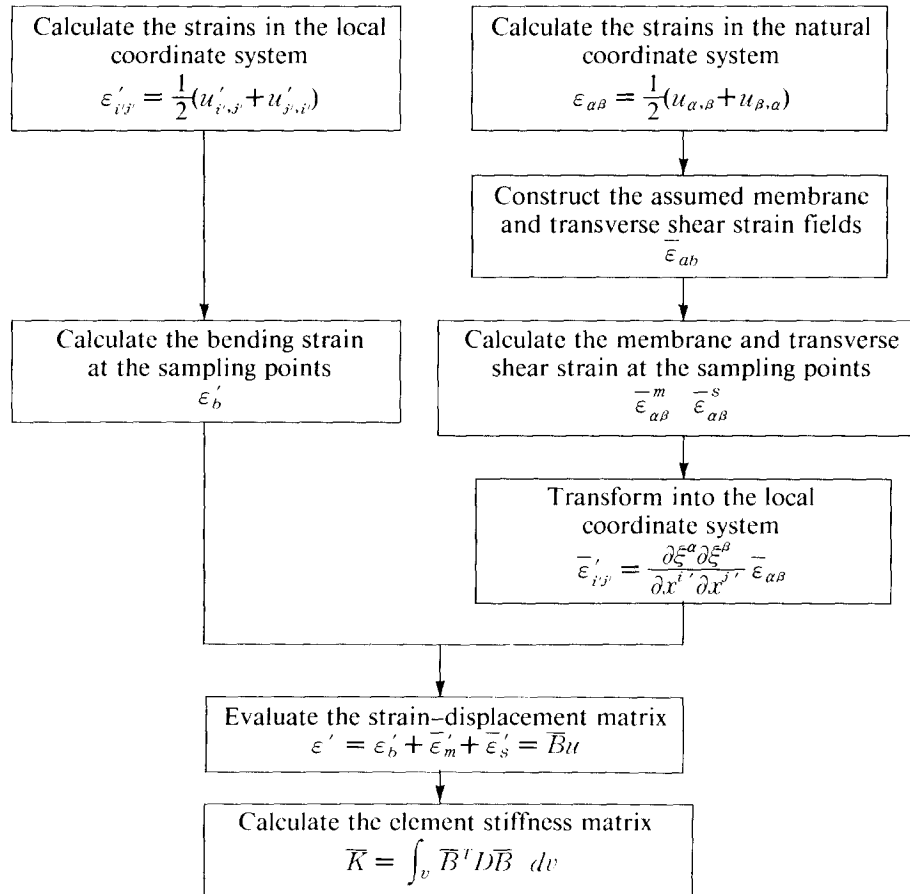


Fig. 1 Procedure of the new element formulation

## 2. The formulation of new four node degenerated shell element

In the contrary to the conventional shell element formulation (Ahmad et al. 1970, Zienkiewicz et al. 1971), the membrane and transverse shear strains are not evaluated from the displacement field but from the assumed covariant strain field in the new element formulation in this study as illustrated in Fig.1.

### 2.1. Geometry Descriptions and Kinematics

The four node degenerated shell element considered here has a quadrilateral shape consisting with four corner nodes as shown in Fig.2(b). The initial geometry of the element can be described by a set of natural coordinates  $(\xi, \eta, \zeta)$  as

$$\begin{Bmatrix} x \\ y \\ z \end{Bmatrix} = \sum_{i=1}^4 N_i(\xi, \eta) \begin{Bmatrix} x_i \\ y_i \\ z_i \end{Bmatrix}_{mid} + \sum_{i=1}^4 N_i(\xi, \eta) \zeta \frac{h_i}{2} \begin{Bmatrix} \bar{v}_{3i}^x \\ \bar{v}_{3i}^y \\ \bar{v}_{3i}^z \end{Bmatrix} \quad (1)$$

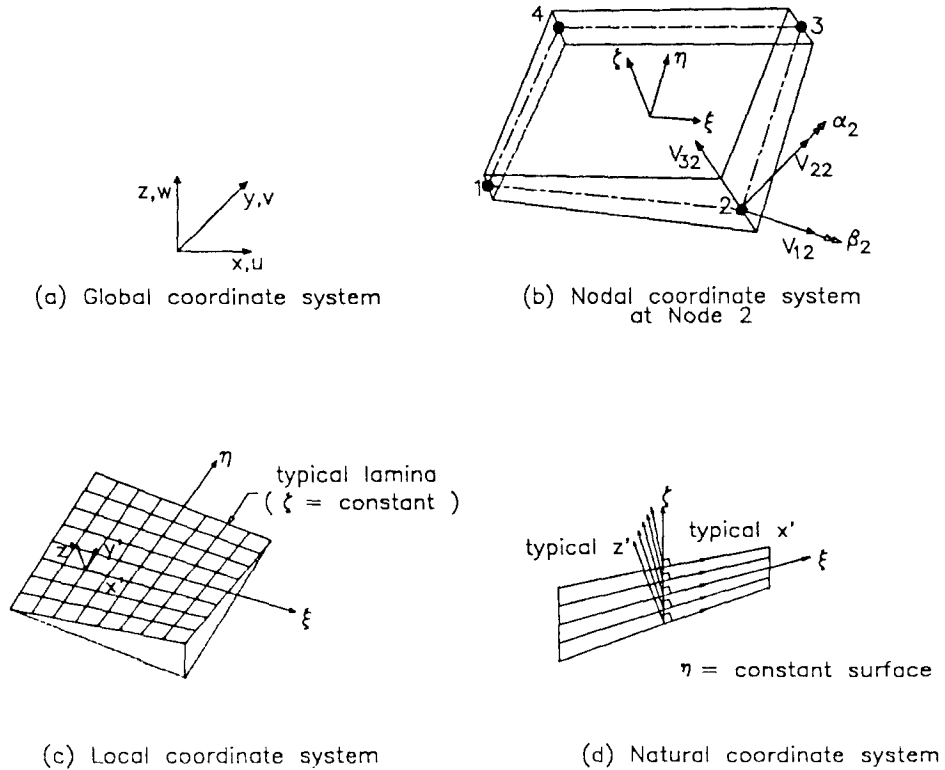


Fig. 2 Element Geometry and Coordinate Systems

where  $N_i(\xi, \eta)$  are the element shape functions corresponding to the surface  $\zeta = \text{constant}$ ,  $h_i$  is the shell thickness at node  $i$ , and  $\xi$ ,  $\eta$ , and  $\zeta$  are the natural coordinates of the point under consideration. The vector  $\mathbf{v}_{3i}$  which is constructed from the nodal coordinates of the top and bottom surface at node  $i$ , thus  $\mathbf{v}_{3i} = \mathbf{x}_i^{top} - \mathbf{x}_i^{bot}$ , where  $\mathbf{x}_i = \langle x_i, y_i, z_i \rangle^T$ . The unit vectors in the directions of  $\mathbf{v}_{3i}$  is represented by  $\bar{\mathbf{v}}_{3i}$ .

At each node in the element, five degrees of freedom are defined, i.e., the three transitional degrees of freedom  $(u, v, w)_i$  in the directions defined by unit vectors  $\mathbf{e}_1$ ,  $\mathbf{e}_2$ ,  $\mathbf{e}_3$  along the global Cartesian axes  $x$ ,  $y$  and  $z$ , respectively, and two rotational degrees of freedom  $\alpha_i$  and  $\beta_i$  which are associated with unit vectors  $\bar{\mathbf{v}}_{2i}$  and  $\bar{\mathbf{v}}_{1i}$ , respectively, defined at node  $i$  as

$$\bar{\mathbf{v}}_{1i} = \frac{\bar{\mathbf{v}}_{3i} \times \mathbf{e}_2}{\|\bar{\mathbf{v}}_{3i} \times \mathbf{e}_2\|}$$

or

$$\bar{\mathbf{v}}_{1i} = -\mathbf{e}_2 \quad \text{if } \|\bar{\mathbf{v}}_{3i} \times \mathbf{e}_2\| = 0 \quad (2)$$

whilst

$$\bar{\mathbf{v}}_{2i} = \bar{\mathbf{v}}_{3i} \times \bar{\mathbf{v}}_{1i}$$

in which  $\|\cdot\|$  denotes the norm of the included vector.

In the kinematics, two assumptions are imposed as only small rotations are considered and nodal fibers are inextensible. Then, the displacement vector  $\mathbf{u} = (u, v, w)$  at a generic point of the shell is expressed in the following form:

$$\begin{Bmatrix} u \\ v \\ w \end{Bmatrix} = \sum_{i=1}^4 N_i \begin{Bmatrix} u_i \\ v_i \\ w_i \end{Bmatrix}_{mid} + \sum_{i=1}^4 N_i \zeta \frac{h_i}{2} \begin{bmatrix} \bar{v}_{1i}^x & -\bar{v}_{2i}^x \\ \bar{v}_{1i}^y & -\bar{v}_{2i}^y \\ \bar{v}_{1i}^z & -\bar{v}_{2i}^z \end{bmatrix} \begin{Bmatrix} \alpha_i \\ \beta_i \end{Bmatrix} \quad (3)$$

## 2.2. Definition of covariant strain components

The covariant displacement components in the natural coordinate system  $\mathbf{u}_a$  are obtained by projecting the displacement components with respect to the global-Cartesian coordinate system  $\mathbf{u}_i$  onto the natural coordinate directions, which is expressed as

$$\mathbf{u}_a = \frac{\partial x^i}{\partial \xi^a} \mathbf{u}_i \quad (\alpha = \xi, \eta, \zeta) \quad (4)$$

where repeated indices imply the summation over the range 1 to 3 ( $x^1 = x$ ,  $x^2 = y$ ,  $x^3 = z$ ,  $u_1 = u$ ,  $u_2 = v$ ,  $u_3 = w$ ). Eq.(4) can also be rewritten in a matrix form as

$$\begin{Bmatrix} u_\xi \\ u_\eta \\ u_\zeta \end{Bmatrix} = \begin{bmatrix} \frac{\partial x}{\partial \xi} & \frac{\partial y}{\partial \xi} & \frac{\partial z}{\partial \xi} \\ \frac{\partial x}{\partial \eta} & \frac{\partial y}{\partial \eta} & \frac{\partial z}{\partial \eta} \\ \frac{\partial x}{\partial \zeta} & \frac{\partial y}{\partial \zeta} & \frac{\partial z}{\partial \zeta} \end{bmatrix} \begin{Bmatrix} u \\ v \\ w \end{Bmatrix} \quad (5)$$

$$= \mathbf{J} \langle u, v, w \rangle^T$$

The derivatives of the covariant displacement in the natural coordinate system are obtained as

$$\begin{bmatrix} \frac{\partial u_\xi}{\partial \xi} & \frac{\partial u_\eta}{\partial \xi} & \frac{\partial u_\zeta}{\partial \xi} \\ \frac{\partial u_\xi}{\partial \eta} & \frac{\partial u_\eta}{\partial \eta} & \frac{\partial u_\zeta}{\partial \eta} \\ \frac{\partial u_\xi}{\partial \zeta} & \frac{\partial u_\eta}{\partial \zeta} & \frac{\partial u_\zeta}{\partial \zeta} \end{bmatrix} = \begin{bmatrix} \frac{\partial u}{\partial \xi} & \frac{\partial v}{\partial \xi} & \frac{\partial w}{\partial \xi} \\ \frac{\partial u}{\partial \eta} & \frac{\partial v}{\partial \eta} & \frac{\partial w}{\partial \eta} \\ \frac{\partial u}{\partial \zeta} & \frac{\partial v}{\partial \zeta} & \frac{\partial w}{\partial \zeta} \end{bmatrix} \mathbf{J}^T \quad (6)$$

The covariant strain components associated with the covariant displacement are defined as

$$\varepsilon_{\alpha\beta} = \frac{1}{2}(u_{\alpha,\beta} + u_{\beta,\alpha}) \quad (\alpha, \beta = \xi, \eta, \zeta) \quad (7)$$

It should be noted that the directions of the covariant strains are equivalent to those of the natural coordinate basis vectors. Detailed expressions for all the covariant strain components are given by

$$\varepsilon_{\xi\xi} = \frac{\partial u_\xi}{\partial \xi} \quad (8a)$$

$$\varepsilon_{\eta\eta} = \frac{\partial u_\eta}{\partial \eta} \quad (8b)$$

$$\varepsilon_{\xi\eta} = \frac{1}{2}\gamma_{\xi\eta} = \frac{1}{2}\left(\frac{\partial u_\xi}{\partial \eta} + \frac{\partial u_\eta}{\partial \xi}\right) \quad (8c)$$

$$\varepsilon_{\xi\zeta} = \frac{1}{2}\gamma_{\xi\zeta} = \frac{1}{2}\left(\frac{\partial u_\xi}{\partial \zeta} + \frac{\partial u_\zeta}{\partial \xi}\right) \quad (8d)$$

$$\varepsilon_{\eta\zeta} = \frac{1}{2}\gamma_{\eta\zeta} = \frac{1}{2}\left(\frac{\partial u_\eta}{\partial \zeta} + \frac{\partial u_\zeta}{\partial \eta}\right) \quad (8e)$$

The terms  $\varepsilon_{\xi\xi}$ ,  $\varepsilon_{\eta\eta}$  and  $\gamma_{\xi\eta}$  are the covariant in-plane strains which are combinations of the membrane and bending behavior. The terms  $\gamma_{\xi\zeta}$  and  $\gamma_{\eta\zeta}$  are the covariant transverse shear strains and the strain in the thickness  $\gamma_{\zeta\zeta}$  is ignored as usual.

### 2.3. Covariant membrane and bending strains

The new element can have non-flat geometry which allows the coupling between the membrane and bending strains. Therefore, in order to define the assumed covariant membrane strains, it is first necessary to decompose the covariant in-plane strains given by Eqs.(8a)–(8c) into the covariant membrane and bending strains.

The total in-plane strains are decoupled into covariant membrane strains and covariant bending strains by defining the covariant membrane strain  $\varepsilon_{\xi\xi}^m$  as the constant part of the covariant in-plane strain  $\varepsilon_{\xi\xi}$  in the  $\zeta$  direction, i.e. the constant covariant in-plane strains at the mid-surface. Similarly, the other covariant membrane strains  $\varepsilon_{\eta\eta}^m$  and  $\gamma_{\xi\eta}^m$  can be defined using  $\varepsilon_{\eta\eta}$  and  $\gamma_{\xi\eta}$ , respectively.

The covariant membrane strains at the Gauss quadrature points through thickness are the same as those at the corresponding mid-surface point. Therefore, as shown in Fig.3, the covar-

inant bending strains at the Gauss quadrature points through thickness are obtained by subtracting the covariant in-plane strains at the mid-surface point from the covariant in-plane strains at the Gauss quadrature points.

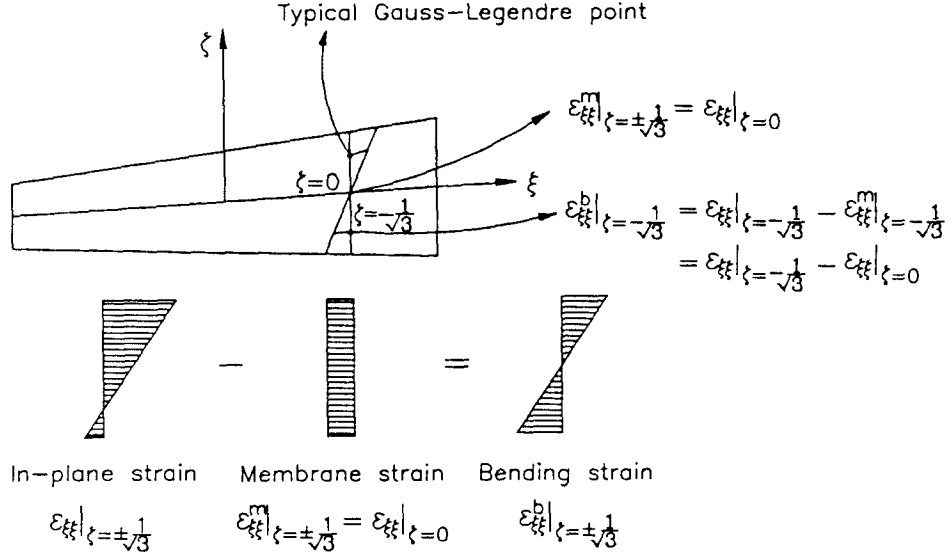


Fig. 3 Covariant membrane strain and bending strain

When compared with other approaches (Park and Stanley 1986, Jang and Pinsky 1987), the proposed method can be more easily implemented, and also include the higher order terms in  $\zeta$  for the covariant bending strains which are neglected in other approaches. Owing to these concepts, this element may become versatile to be applied to a wide range of shell problems, i. e., thin, thick and laminated composite shells.

#### 2.4. Determination of assumed covariant strain field

The derivation of the assumed covariant strain field for the four node shell element proceeds as follow. Covariant strain components are evaluated along the four element sides which are called the *natural coordinate lines*. The assumed covariant strain field can then be calculated through the appropriate interpolation of covariant strain components in the two interpolation directions over the element as shown in Fig.4. The values of  $\bar{\epsilon}^m_{\xi\xi}$  and  $\bar{\gamma}^m_{\xi\zeta}$  on the natural coordinate lines are interpolated through the  $\eta$ -direction, and  $\bar{\epsilon}^m_{\eta\eta}$  and  $\bar{\gamma}^m_{\eta\zeta}$  are also interpolated through  $\xi$ -direction while the membrane shear strain  $\bar{\gamma}^m_{\xi\eta}$  is interpolated in both directions. Linear interpolations are used for all strain components except the membrane shear strain. It is well known that the full integration (2-point quadrature) for the transverse shear and membrane strains along the natural coordinate lines cause the locking (Park and Stanley 1986, Huang and Hinton 1986). Therefore, the integration points for both strains should be chosen to avoid this locking. For this purpose, this paper presents an appropriate integration points in the following two sections.

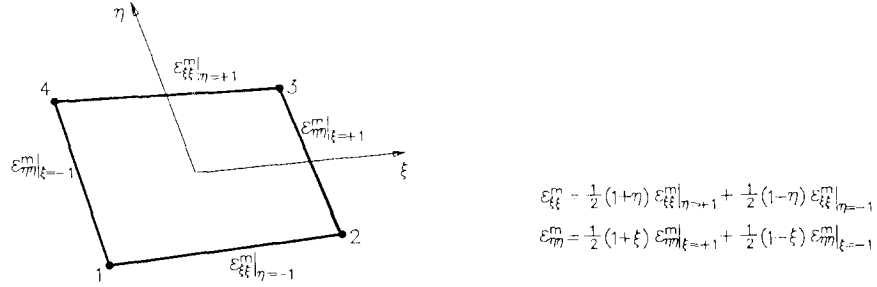


Fig. 4 Natural coordinate lines and interpolation functions

#### 2.4.1. Covariant transverse shear strain along the natural coordinate lines

To determine the covariant transverse shear strain field to avoid the shear locking, we consider a natural coordinate line  $\eta = +1$ . Then, this natural coordinate line is considered as a Timoshenko beam connected between nodes 3 and 4. Using the Timoshenko beam theory, the strain energy can be written as:

$$U = \frac{1}{12} E h^3 \int \kappa_{,\xi}^2 d\xi + \frac{G h \phi}{2} \int \gamma_{\xi\zeta}^2 d\xi \quad (9)$$

where  $\kappa_{,\xi} = \theta_{,\xi}$  is the section curvature and  $\gamma_{\xi\zeta} = w_{,\xi} + \theta$  is the transverse shear strain. In Eq. (9),  $E$ ,  $G$  are Young's modulus and the shear modulus, respectively.  $h$  is the shell thickness and  $\phi$  is the shear correction factor.

In a  $C^0$  beam element, the displacement and rotation field are approximated in terms of the natural coordinate  $\xi$  as follows:

$$\begin{aligned} w(\xi) &= \sum_{i=1}^2 N_i(\xi) w_i \\ \theta(\xi) &= \sum_{i=1}^2 N_i(\xi) \theta_i \end{aligned} \quad (10)$$

where  $w_i$  and  $\theta_i$  are the nodal displacements and rotations, respectively, and  $N_i$  are the related shape functions as follows:

$$\begin{aligned} N_1 &= \frac{1}{2}(1-\xi) \\ N_2 &= \frac{1}{2}(1+\xi) \end{aligned} \quad (11)$$

The curvature and transverse shear strain emanating from Eq.(11) is then obtained in the following form:

$$\begin{aligned} \kappa_{,\xi} &= \theta_{,\xi} = [B_r] \{d\} \\ \gamma_{\xi\zeta} &= w_{,\xi} + \theta = [B_s] \{d\} \end{aligned} \quad (12)$$



where

$$\begin{aligned}\{d\} &= [w_1, \theta_1, w_2, \theta_2] \\ [B_f] &= [0, N_{1,\xi}, 0, N_{2,\xi}] = \left[ 0, -\frac{1}{2}, 0, \frac{1}{2} \right] \\ [B_s] &= [N_{1,\xi}, N_1, N_{2,\xi}, N_2] = \left[ -\frac{1}{2}, \frac{1}{2}(1-\xi), \frac{1}{2}, \frac{1}{2}(1+\xi) \right]\end{aligned}$$

The curvature is a constant given by

$$\kappa_\xi = \frac{(\theta_2 - \theta_1)}{2} \quad (13)$$

while the transverse shear strain has the following linear variation along the element:

$$\gamma_{\xi\zeta} = A + B\xi \quad (14)$$

where

$$\begin{aligned}A &= \frac{(w_2 - w_1)}{2} + \frac{(\theta_2 + \theta_1)}{2} \\ B &= \frac{(\theta_2 - \theta_1)}{2}\end{aligned}$$

As the beam span-to-thickness ratio ( $L/h$ ) approaches to infinity, the Euler (Kirchhoff) constraints are also enforced to approach to zero ( $A \rightarrow 0$ ,  $B \rightarrow 0$ ) over the entire element domain (Donea and Lamain 1987, Tessler and Hughes 1983).

The condition on  $A=0$  means physically that the average element rotation equals to the element slope, which is clearly satisfied for slender beams. On the other hand,  $B=0$  imposes a uniform or zero rotation on the element. This constraint leads to vanishing of the section curvature ( $\kappa_\xi$  in Eq.(13)) and the bending energy, and thus leads as to shear locking. At this point it is apparent that the linear term in the shear strain polynomial ( $B$  in Eq.(14)) must be removed to permit the condition of vanishing shear strains in thin beam limit to be attained without engendering spurious constraining. Therefore, the transverse shear strain in a linear  $C^0$  beam must be rendered elementwise constant. To achieve this, consider the modified transverse shear strain corresponding to the mean value of the original transverse shear strain over the element.

$$\bar{\gamma}_{\xi\zeta} = \frac{(w_2 + w_1)}{2} + \frac{(\theta_2 + \theta_1)}{2} \quad (15)$$

The limiting condition of vanishing transverse shear strains is now clearly attainable without any spurious constraining.

It should be noted that the transverse shear strain values obtained from the original polynomial and those from the modified polynomial coincide at the one-point Gaussian integration station ( $\xi=0$ ) as shown in Fig.5. Hence, the assumed covariant transverse shear strain along the natural coordinate line  $\eta = \pm 1$  is obtained with a one-point integration of the original linear transverse shear strain polynomial. Similar expression can be obtained for  $\bar{\gamma}_{\eta\zeta}$  by simply interchanging  $\xi$  by  $\eta$  in  $\bar{\gamma}_{\xi\zeta}$ . Therefore, the assumed covariant transverse shear strain  $\bar{\gamma}_{\xi\zeta}$  is constant in  $\xi$  and linear in  $\eta$ . Conversely, the assumed covariant transverse shear strain  $\bar{\gamma}_{\eta\zeta}$  is constant in  $\eta$  and linear in  $\xi$ . The assumed covariant transverse shear strain field is given in Fig.6.

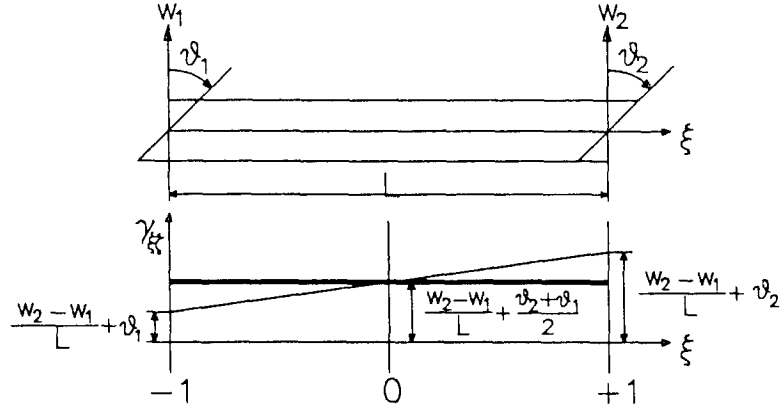


Fig. 5 Assumed covariant transverse shear strain along the natural coordinate line

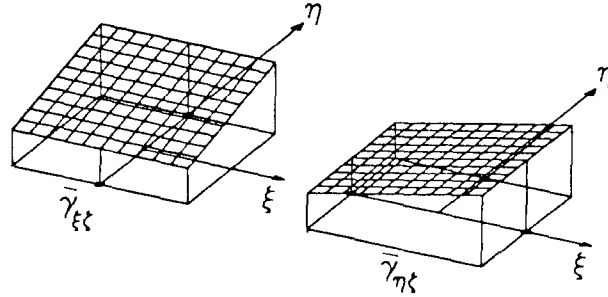


Fig. 6 Assumed covariant transverse shear strain fields

#### 2.4.2. Covariant membrane strain along the natural coordinate lines

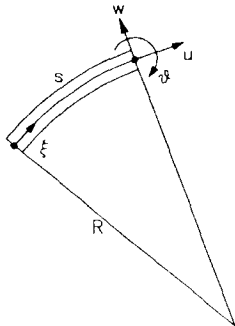


Fig. 7 Geometry of curved Timoshenko beam

To determine the covariant membrane strain field, we shall consider a arch Timoshenko beam (Tessler and Hughes 1983) in Fig.7 to examine the membrane action in the beam. The strain energy of this element may be written as

$$U = \int \frac{EA}{2} (u_{,\xi} + \frac{w}{R})^2 d\xi + \int \frac{EI}{2} \theta_{,\xi}^2 d\xi + \int \frac{GA\phi}{2} (\theta + w_{,\xi})^2 d\xi \quad (16)$$

Considering the effects due to the introduction of these simple shape functions into the membrane strains, the displacements can be written as

$$\begin{aligned} u &= a_1 + a_2 \xi \\ w &= b_1 + b_2 \xi \end{aligned} \quad (17)$$

so that the membrane strain  $\bar{\varepsilon}_{\xi\xi}^m$  becomes

$$\bar{\varepsilon}_{\xi\xi}^m = u_{,\xi} + \frac{w}{R} = \left( a_2 + \frac{b_1}{R} \right) + \frac{b_2}{R} \xi \quad (18)$$

When arch beam is subjected to a state of pure bending, the membrane strain will vanish. Therefore, an inextensional bending that will enforce the following constraints is expected

$$\begin{aligned} a_2 + \frac{b_1}{R} &= 0 \\ \frac{b_2}{R} &= 0 \end{aligned} \quad (19)$$

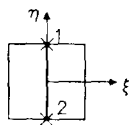
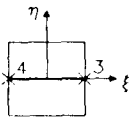
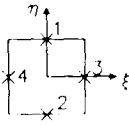
Clearly, the second constraint in Eq.(19) would introduce a spurious in-plane stiffening state that was described as membrane locking, which was demonstrated for the curved and arch beams (Belytschko et al. 1985, Prathap 1985). Therefore, to eliminate the spurious constraint, the membrane strains must be made elementwise constant as in the transverse shear strains.

Hence, the assumed covariant membrane strain along the natural coordinate lines  $\eta = \pm 1$  is obtained by a one-point integration of the original linear membrane strain polynomial. Similar expression can be obtained for  $\bar{\varepsilon}_{\eta\eta}^m$  by interchanging  $\xi$  by  $\eta$  in  $\bar{\varepsilon}_{\xi\xi}^m$ .

The assumed covariant membrane shear strain  $\bar{\gamma}_{\xi\eta}^m$  is defined as a pure constant distribution to improve membrane bending performance of the element. This strain is obtained by averaging the covariant membrane shear strains at one-point integration along the natural coordinates ( $\xi = \pm 1, \eta = \pm 1$ ).

For the assumed covariant strain fields, interpolation functions and interpolation points are used as shown in Table 2.

Table 2 Interpolation function

Interpolation Directions	Strains	Interpolation Functions
	$\bar{\varepsilon}_{\xi\xi}^m$ $\bar{\gamma}_{\xi\xi}$	$N_1 = \frac{1}{2}(1 + \eta)$ $N_2 = \frac{1}{2}(1 - \eta)$
	$\bar{\varepsilon}_{\eta\eta}^m$ $\bar{\gamma}_{\eta\eta}$	$N_3 = \frac{1}{2}(1 + \xi)$ $N_4 = \frac{1}{2}(1 - \xi)$
	$\bar{\gamma}_{\xi\eta}^m$	$S_1 = S_2 = S_3 = S_4 = \frac{1}{2}$

### 2.5. Substituted strain – displacement matrix

The assumed covariant membrane and shear strain at the Gauss quadrature points are obtained using the aforementioned assumed covariant membrane and shear field. And local Cartesian strains may then be obtained from these strains by the use of the following tensor transformation:

$$\bar{\varepsilon}_{i'j'} = \frac{\partial \xi^\alpha}{\partial x^{i'}} \frac{\partial \xi^\beta}{\partial x^{j'}} \bar{\varepsilon}_{\alpha\beta} \quad (i', j' = x', y', z') \quad (20)$$

where repeated indices imply summation over the range 1 to 3 ( $\xi^1 = \xi$ ,  $\xi^2 = \eta$ ,  $\xi^3 = \zeta$ ).

Therefore, the strain–displacement matrix **B**, relating the strain components in the local coordinate system to the element nodal variables, can be constructed. Obtaining the element stiffness matrix is now straight forward.

## 3. Numerical Examples

A number of commonly used benchmark problems are examined to compare the present element with other element models in the open literature to assess their relative accuracy and convergence. Elements to be included in the comparisons are summarized in Table 3.

Table 3 Summary of elements used in comparisons

Name	Element Description
4-SRI	Four node shell element with selective reduced integration on the transverse shear terms. This element possesses two zero energy modes (Belytschko et al. 1989).
4-URI	Four node shell element with uniformly reduced integration. This element possesses six zero energy modes (Belytschko et al. 1989).
4-RSDS	Four node resultant stress degenerated shell element (Belytschko et al. 1989).
4-Bathe	Four node shell element based on assumed shear strain field (Dvorkin and Bathe 1984).
4-ANS	Four node shell element based on assumed covariant strains (Park and Stanley (1986).

In addition to some standard examples which illustrate the convergence in displacements, we have included problems which are designed to demonstrate the convergence in stresses obtained from the proposed shell element, including transverse shear stress. These examples show not only that the new shell element is accurate in all stress components but also that these stresses do not significantly deteriorate with mesh distortion.

### 3.1. Eigenvalue analysis

The element stiffness matrix of the proposed element was such that the number of zero eigenvalues are only the six modes corresponding to the six rigid body motions, thus this element was identified not to include any spurious singular modes.

### 3.2. Square plate problem for perturbed meshes

The problem suggested by Lasry and Belytschko(1987) is tested to observe the oscillations in the transverse shear stress under mesh perturbations. This problem involves a clamped square plate of dimension 10 and thickness of 0.1. Young's modulus of the material is  $1.092 \times 10^6$  and Poisson's ratio is 0.3. Only a quarter of the plate was actually analyzed due to the symmetry of the structure. Six nodes per side were employed in generating the mesh as shown in Fig.8. A perturbation was introduced at node A, which has coordinates (3.0,3.0) in the regular mesh and (3.1, 2.9) in the perturbed mesh. Results for transverse shear forces  $Q_{xz}$  and  $Q_{yz}$  along the lines  $y=1.5$  in this study are plotted in Fig.9 along with an analytical solution (MacNeal and Harder 1985). These figures show that the severe oscillations in transverse shear forces obtained by using 4-SRI elements (Lasry and Belytschko 1987) and that the proposed element is unaffected by the perturbation.

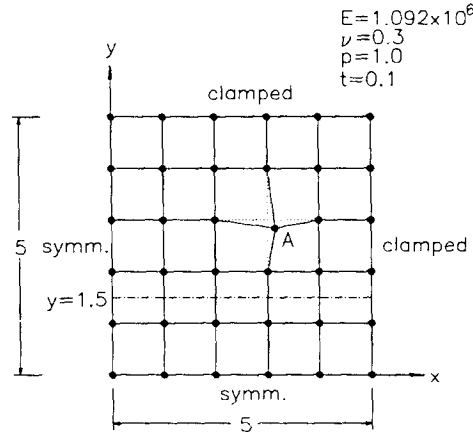


Fig. 8 Square plate for perturbed meshes

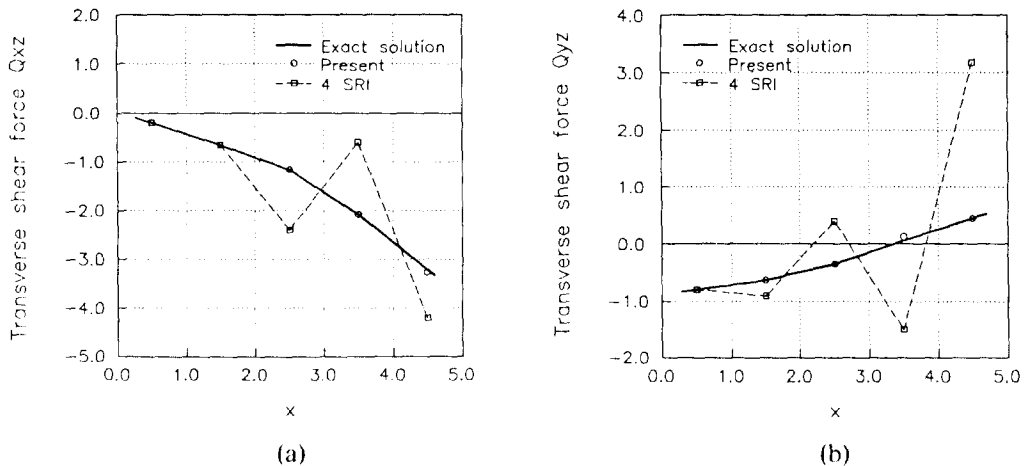


Fig. 9 Shear forces  $Q_{xz}$  and  $Q_{yz}$  along line  $y=1.5$

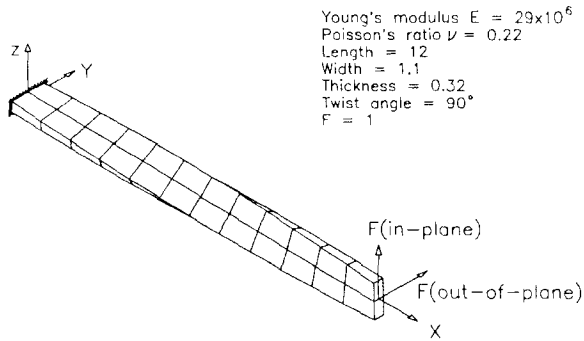


Fig. 10 Twisted beam

Table 4 Normalized solution for twisted beam

Direct. of Load	In-Plane		Out-of-Plane	
	Nodes/Side	3×13	5×25	3×13
4-SRI	0.995	0.998	0.924	0.976
4-URI	1.009	1.001	1.076	1.014
4-RSDS	1.436	1.411	1.377	1.361
4-Bathe	0.988	0.996	0.920	0.974
Present	0.994	0.998	0.982	0.994

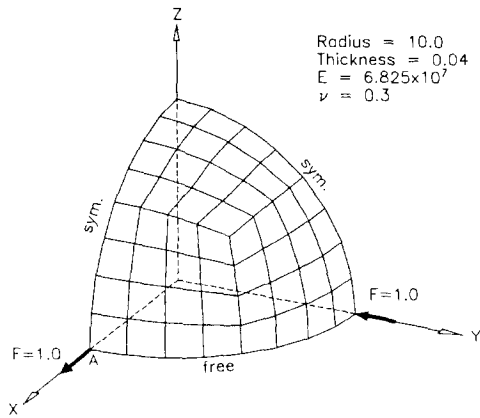


Fig. 11 Hemispherical shell problem

Table 5 Results for hemispherical shell

Nodes/Side	4-SRI	4-URI	4-RSDS	4-Bathe	4-ANS	Present
5	0.412	1.048	0.965	0.372	0.01	1.027
9	0.927	0.993	0.971	0.920	0.05	1.002
17	0.984	1.00	0.989	0.990	0.120	0.996

$R = 25.0$   
 $L = 50.0$   
Thickness = 0.25  
 $E = 4.32 \times 10^8$   
 $\nu = 0.0$   
Weight = 90.0 per unit area

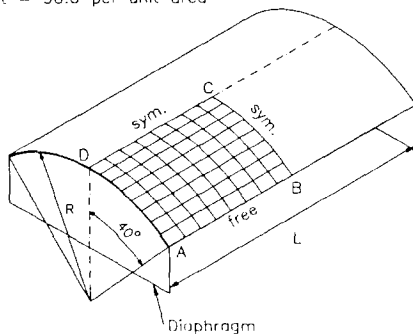


Fig. 12 Scordelis-Lo roof problem

Table 6 Results for Scordelis-Lo roof problem

Nodes/Side	4-SRI	4-URI	4-RSDS	4-Bathe	Present
5	0.964	1.219	1.201	0.944	1.044
9	0.984	1.054	1.046	0.973	1.002
17	0.999	1.017	1.011	0.989	0.995

### 3.3. Twisted cantilever beam problem

A cantilever beam of rectangular cross-section, twisted  $90^\circ$  over its length, is subjected to a concentrated unit load at its free end as shown in Fig.10. This problem was proposed to assess the effect of the element warping distortion. The analytic solutions in the direction of the in-plane load and that of the out-of-plane load are  $0.5424 \times 10^{-2}$  and  $0.1754 \times 10^{-2}$ , respectively, as quoted in MacNeal and Harder (1985). The displacements in the direction of the applied loading are given in Table 4. They have been normalized with respect to the analytic solutions.

The proposed element could include the correct warping effect and do not suffer from locking. All the elements tested, i.e., 4-SRI, 4-URI, 4-Bathe and the proposed element, show the reasonable convergence to the analytic solution in the direction of in-plane load. However, the proposed element yields a better convergence than 4-SRI and 4-Bathe in direction of out-of-plane load.

### 3.4. Hemispherical shell problem

A hemispherical shell subjected to self-equilibrating radial point forces at  $90^\circ$  intervals, is analyzed via the quarter model shown in Fig. 11. This problem is intended to check the element performance for the rigid body rotations and the near inextensional bending of a doubly curved shell. The geometry and material properties are shown in Fig.11. An analytical solution for the problem is given by Flugge (1973). The analytic solution for the radial displacement at the loaded points is 0.0924. One quarter of the hemisphere was actually analyzed using the symmetry of the structure. Results for different mesh sizes are presented in Table 5. They indicate that the proposed element performs well, while 4-ANS element is locked due to the rigid body straining (Stanley 1985).

### 3.5. Scordelis-Lo roof problem under gravity load

This problem is the membrane dominated example involving very little inextensional bending. The roof subtends an angle of  $80^\circ$  and the roof is subjected to a distributed gravity load of 90 per unit area.

The geometry of the problem is given in Fig.12. The material has a Young's modulus of  $4.32 \times 10^6$  and Poisson's ratio of 0.0. The roof is supported at each end by rigid diaphragms. An analytical solution for the transverse displacement at the center of the roof edge(C), as reported by MacNeal and Harder (1985), is 0.3024. Using the symmetry of the problem, only a quarter of the roof was analyzed. Normalized values for transverse displacement at C are given in Table 6, for various mesh sizes. All the reported elements do quite well for this example, but it can be seen that the proposed element is more accurate than the other elements. Figs. 13 and 14 compare the vertical displacements on the mid-section and the longitudinal displacements at diaphragm to the exact shallow shell solution. Good results are obtained with  $8 \times 8$  mesh per one-quarter of the roof.

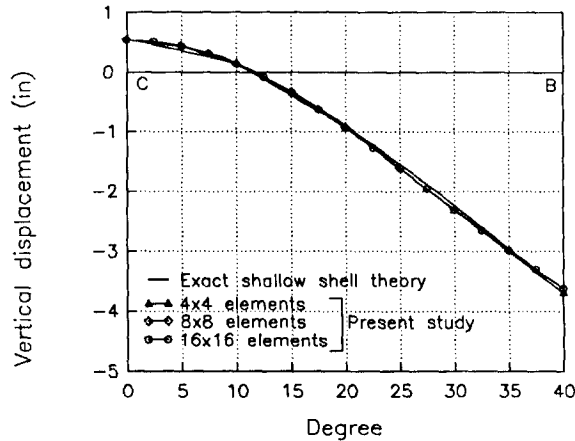


Fig. 13 Vertical displacement on the mid-section

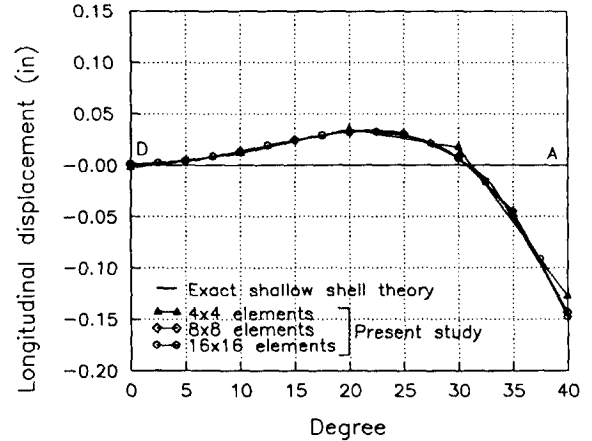


Fig. 14 Longitudinal displacement at diaphragm

### 3.6. Pinched cylinder problem

The pinched cylinder is a classical problem that has been used extensively to check the ability of shell elements to represent the inextensional bending deformation. The open-end cylinder leads to the pure inextensional deformation at the limit as  $t/R$  approaches zero. An analytic solution for this limiting case is given by Timoshenko and Woinwky-Krieger (1959) which is 0.1139. Fig.15 shows the model geometry. Using symmetry only one eighth of the cylinder was actually analyzed. Normalized transverse displacements under the load are given Tables 7 for different mesh sizes. Numerical results for the pinched cylinder with open ends indicate that the proposed element exhibits a good accuracy.

Considering the stresses for the pinched cylinder with rigid end diaphragms predicted in Figs.16–17 which are stresses at the element centroids, a good overall accuracy of the proposed element is clearly seen.

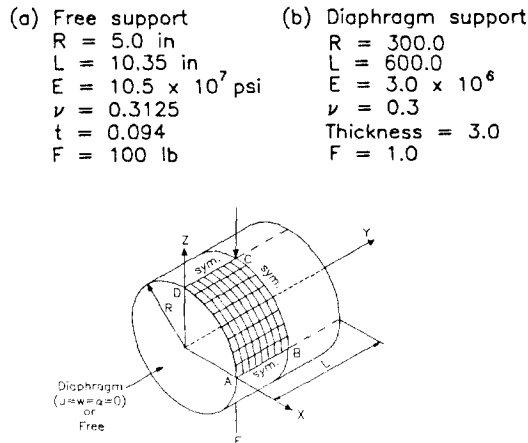


Fig. 15 Pinched cylinder problem

Table 7 Results for pinched cylinder cylinder with free ends

Nodes/ Side	4-SRI 4-ANS	4-RSDS	4-Bathe	Present
3	0.634	1.065	0.753	0.754
5	0.904	0.931	0.943	0.944
9	0.992	0.997	1.002	1.003
17	1.019	1.020	1.020	1.020



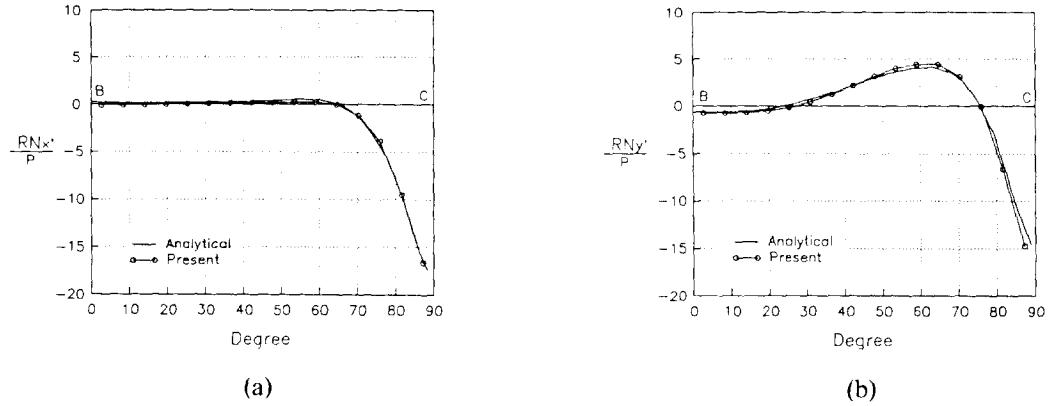


Fig. 16 Distributions of membrane stresses along BC for a pinched cylinder with  $16 \times 16$  mesh

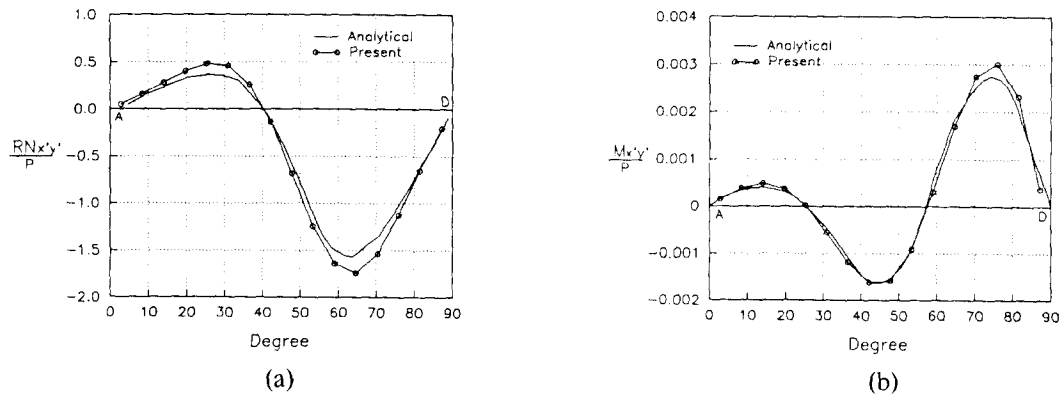


Fig. 17 Distributions of membrane shear and twisting moment along AD for a pinched cylinder with  $16 \times 16$  mesh

#### 4. Conclusion

A new formulation for a four node shell element based on the assumed strain method is proposed in this study.

To avoid the shear locking in shell problems, the element uses the assumed covariant shear strains. The assumed covariant membrane strains which are separated from the covariant in-plane strains by mid-surface interpolation, are applied to alleviate the membrane locking problem and also to improve the membrane bending performance.

The new element which has no spurious zero energy modes can be effectively applied to a wide range of shell modeling, i.e., thin, thick and laminated composite shells.

Numerical results show that this new element has a rapid convergence and provides a reasonable accuracy in the stress prediction. This element was also found to be free of membrane and shear locking problems, and thus improved the overall membrane bending behavior of the shell.

## References

- Ahmad, S., Irons, B.M. and Zienkiewicz, O.C. (1970), "Analysis of thick and thin shell structures by curved finite elements", *Int. J. Num. Meth. Engng*, **2**, 419–451.
- Bathe, K.J. and Dvorkin, E.N. (1986), "A formulation of general shell elements—the use of mixed interpolation of tensorial components", *Int. J. Num. Meth. Engng*, **22**, 697–722.
- Belytschko, T., Stolarski, H. and Liu, W.K. (1985), "Stress projection for membrane and shear locking in shell finite elements", *Comp. Meth. App. Mech. Engng*, **51**, 221–258.
- Belytschko, T., Wong, B.L. and Stolarski, H. (1989), "Assumed strain stabilization procedure for 9-node la-grange shell element", *Int. J. Num. Meth. Engng*, **28**, 385–414.
- Choi, C.K. and Kim, S.H. (1989), "Coupled use of reduced integration and nonconforming modes in quadratic Mindlin elements", *Int. J. Num. Meth. Engng*, **28**, 1909–1929.
- Donea, J. and Lamain, L.G. (1987), "A modified representation of transverse shear in  $C^0$  quadrilateral plate elements", *Comp. Meth. App. Mech. Engng*, **63**, 183–207.
- Dvorkin, E.N. and Bathe, K.J. (1984), "A continuum mechanics based four-node shell element for general nonlinear analysis", *Engng Comput.*, **1**, 77–88.
- Flugge, W. (1973), *Stresses in shells*, 2nd edition, Springer, Berlin.
- Hughes, T.T.R. and Cohen, M. (1978), The heterosis finite element for plate bending, *Comp. Struct.*, **9**, 445–50.
- Hughes, T.T.R., Cohen, M. and Haroun, M. (1978), "Reduced and selective integration techniques in the finite element analysis of plates", *Nuclear Engineering and Design*, **46**, 203–222.
- Huang, H.C., (1987), "Membrane locking and assumed strain shell elements", *Comp. Struct.*, **27**, 671–677.
- Huang, H.C. and Hinton, E. (1986), "A new nine node degenerated shell element with enhanced membrane and shear interpolation", *Int. J. Num. Meth. Engng*, **22**, 73–92.
- Jang, J. and Pinsky, P.M. (1987), "An assumed covariant based 9-node shell element", *Int. J. Num. Meth. Engng*, **24**, 2389–2411.
- Lasry, D. and Belytschko, T. (1987), "Transverse shear oscillation in four-node quadrilateral plate elements", *Comp. Struct.*, **27**, 393–398.
- Lee, S.W. and Pain, T.H.H. (1978), "Improvement of plate and shell finite elements by mixed formulations", *AIAA Journal*, **16**, 29–34.
- MacNeal, R.H. and Harder, R.L. (1985), "A proposed standard set of problems to test finite element accuracy", *Finite Elements in Analysis and Design*, **1**, 3–20.
- Parisch, H. (1979), "A critical survey of the 9-node degenerated shell element with special emphasis on thin shell applications and reduced integration", *Comp. Meth. App. Mech. Engng*, **20**, 323–250.
- Park, K.C. and Stanley, G.M. (1986), "A curved  $C^0$  shell element based on assumed natural-coordinate strains", *J. of Applied Mechanics, ASME*, **53**, 278–290.
- Prathap, G. (1985), "A  $C^0$  continuous four-noded cylindrical shell element", *Comp. Struct.*, **21**, 995–999.
- Stanley, G.M. (1985), *Continuum-based shell analysis*, Ph.D. Dissertation, Stanford University, Stanford, California.
- Tessler, A. and Hughes, T.J.R. (1983), "An improved treatment of transverse shear in the Mindlin-type four-node quadrilateral element", *Comp. Meth. App. Mech. Engng*, **39**, 311–335.
- Timoshenko, S. and Woinowsky-Krieger, S. (1959), *Theory of Plate and Shells*, 2nd Edition, McGraw-Hill, New York.
- Zienkiewicz, O.C., Taylor, R.L. and Too, J.M. (1971), "Reduced integration technique in general analysis of plates and shells", *Int. J. Num. Meth. Engng*, **3**, 275–290.